Aib-Rich Peptides Containing Lactam-Bridged Side Chains as Models of the 3_{10}-Helix

Elisabetta Schievano,[†] Alessandro Bisello,[‡] Michael Chorev,[‡] Arianna Bisol,[†] Stefano Mammi,[†] and Evaristo Peggion*[,†]

Contribution from the University of Padova, Department of Organic Chemistry, Biopolymer Research Center, C.N.R, Via Marzolo 1, 35131 Padova, Italy, and Division of Bone and Mineral Metabolism, Charles A. Dana Thorndike Laboratories, Beth Israel Deaconess Medical Center, Harvard Medical School, 330 Brookline Avenue, Boston, Massachusetts, 02215

Received July 24, 2000. Revised Manuscript Received December 15, 2000

Abstract: Aib-rich side chain lactam-bridged oligomers Ac−(Glu-Aib-Aib-Lys)$_n$-Ala-OH, with n =1, 2, 3, were designed and synthesized as putative models of the 3_{10}-helix. These peptides were conformationally characterized in aqueous solution containing SDS micelles by CD, NMR, and computer simulations. The lactam bridge between the side chains of L-Glu and L-Lys in (*i*) and (*i*+*3*) positions was introduced in order to enhance the conformational preference toward the right-handed 3_{10}-helix. The NMR results clearly indicate that there is an increase of 3_{10}-helix formation upon chain elongation. In the dimer and trimer (n = 2 and n = 3, respectively, in the structure reported above) the observed NOE connectivities are compatible with the 3_{10}-helical arrangement, confirmed by the temperature coefficients of the amide proton resonances which suggest the presence of a hydrogen-bonded structure. The ϕ and ψ dihedral angles of the structures obtained by molecular dynamics calculations are also compatible with the 3_{10}-helix. Identification of the hydrogen-bond pattern indicate that C═O(*i*)- - -HN(*i*+3) hydrogen bonds, typical of the 3_{10}-helical conformation, are highly probable in all low-energy structures. The CD spectra of these Aib-rich lactam-bridged oligopeptides, obtained in the same solvent system used for NMR experiments, provide important insight into the spectroscopic characteristics of the 3_{10}-helix.

Introduction

The 3_{10}-helix, besides the classical α-helix and β-pleated sheet conformations, represents an important secondary structural element occurring in globular proteins. The 3_{10}-helices are in general shorter than the α-helices or appear at the termini of α-helices where the altered hydrogen-bond (H-bond) pattern provides some helix capping.[1] It has also been suggested that short 3_{10}-helices can serve as nucleation sites in helix formation during protein folding. There is therefore a significant interest in the 3_{10}-helix structure. Such a conformation has been described at atomic resolution in model peptides and peptaibol antibiotics.[2] Oligopeptides rich in Aib (α-aminoisobutyric acid) residues or, in general, in C^{α}-tetra-substituted amino acids exhibit a strong preference toward the formation of a 3_{10}-helix.[2] This structure has been observed either in the crystal state by X-ray diffraction techniques[3] or in solution using FT-IR absorption and vibrational CD spectroscopy.[4−8] Electronic CD and NMR are the most extensively used spectroscopic tools to elucidate secondary structures of peptides. In general, the spectroscopic differentiation of the 3_{10}-helix from the classical α-helix is a difficult problem because the conformational parameters of the two structures are very similar. Indeed, the ϕ and ψ backbone dihedral angles of the two helices differ only by 6° and 12°, respectively, and the 3_{10}-helix is just slightly more elongated than the α-helix[2]. Using NMR spectroscopy, the only medium-range NOEs which can be used to distinguish between the two helices are the $d_{\alpha N}(i,i+2)$ and the relative intensities of the $d_{\alpha N}(i,i+n)$ cross-peaks for n = 2, 3, 4. However, $d_{\alpha N}(i,i+2)$ NOEs are also observed in β-turns and can result in a system where α-helices are in dynamic equilibrium with unfolded forms.[9] Quite recently, the groups of Kessler and Toniolo[10] characterized the heptapeptide *m*BrBz[Iva-(αMe)-Val]$_2$-(αMe)Phe-(αMe)Val-Iva-NH-Me (*m*BrBz, *meta*-bromobenzoyl; Iva, isovaline; (αMe)Val, C^{α}-methyl valine; αMe-Phe, C^{α}-methyl phenylalanine; NH-Me, *N*-methyl amide) by combined X-ray diffraction and NMR analysis and restrained molecular dynamics (MD) simulations. The authors showed that, in the crystal state, the N-terminally acylated heptapeptide

* To whom correspondence should be addressed. Dr. E. Peggion, Department of Organic Chemistry, University of Padova, Biopolymer Research Center, Via Marzolo 1, 35131 Padova, Italy, Telephone: 39/049/827-5262. Fax: 39/049/827-5239. E-mail: peggion@chor.unipd.it.

† University of Padova.

‡ Harvard Medical School.

(1) Barlow, D. J.; Thornton, J. M. *J. Mol. Biol.* **1988**, *201*, 601−619.

(2) Toniolo, C.; Benedetti, E. *Trends Biochem. Sci.* **1991**, *16*, 350−353.

(3) Toniolo, C.; Crisma, M.; Formaggio, F.; Valle, G.; Cavicchioni, G.; Précigoux, G.; Aubry, A.; Kamphuis, J. *Biopolymers* **1993**, *33*, 1061−1072.

(4) Yoder, G.; Keiderling, T. A.; Formaggio, F.; Crisma, M.; Toniolo, C.; Kamphuis, J. *Tetrahedron: Asymmetry* **1995**, *6*, 687−690.

(5) Yasui, S. C.; Keiderling, T. A.; Bonora, G. M.; Toniolo, C. *Biopolymers* **1986**, *25*, 79−89.

(6) Bour, P.; Keiderling, T. A. *J. Am. Chem. Soc.* **1993**, *115*, 9602−9607.

(7) Yasui, S. C.; Keiderling, T. A.; Formaggio, F.; Bonora, G. M.; Toniolo, C. *J. Am. Chem. Soc.* **1986**, *108*, 4988−4993.

(8) Yoder, G.; Keiderling, T. A.; Formaggio, F.; Crisma. M.; Toniolo, C. *Biopolymers* **1995**, *35*, 103−111.

(9) Andersen, N. H.; Liu, Z.; Prickett, K. S. *FEBS Lett.* **1996**, *399*, 47−52.

(10) Gratias, R.; Konat, R.; Kessler, H.; Crisma, M.; Valle, G.; Polese, A.; Formaggio, F.; Toniolo, C.; Broxterman, Q. B.; Kamphuis, J. *J. Am. Chem. Soc.* **1998**, *120*, 4763−4770.

10.1021/ja0027261 CCC: $20.00
Published on Web 03/03/2001

methylamide adopts a regular, right-handed 3_{10}-helical structure. On the basis of NMR results obtained in $CDCl_3$ and the related restrained MD calculations, the authors concluded that the 3_{10}-helix is the predominant structure present in solution.

A debated problem is whether the α- and 3_{10}-helical structures can be distinguished by CD spectroscopy in the amide absorption region. Manning and Woody,[11] on the basis of a detailed theoretical study, concluded that the CD pattern of the 3_{10}-helix differs from that of an α-helix in the ratio of the intensities of the two negative bands at 222 and 208 nm (~1 for α-helix and much lower for the 3_{10}-helix). Balaram and co-workers[12] experimentally studied a series of helical peptides ranging from 10 to 21 amino acid residues and concluded that the two helical structures cannot be distinguished by CD. This view was also supported by CD studies by Andersen et al.[9] of pancreatic amylin analogues containing up to five Aib residues.

More recently, Toniolo and co-workers[13,14] carried out a systematic study of Nα-protected L-(αMe)Val homo-oligomers in the solid state and in various solvent systems. The Nα-protected *Z*-[L-(αMe)Val]$_8$-O*t*Bu (*Z*, benzyloxycarbonyl; O*t*Bu, *tert*-butylester) oligomer is completely in the 3_{10}-helical structure in the crystal state.[14] In addition, detailed FT-IR absorption studies, supported by solvent accessibility measurements of NH protons by NMR, indicated that this octapeptide folds into the right-handed 3_{10}-helix in $CDCl_3$ solution. The CD spectrum reported by Toniolo et al.[14] in TFE (2,2,2-trifluorethanol), where the peptide supposedly assumes the same conformation as in $CDCl_3$, displays a negative CD band at 207 nm and a shoulder around 222 nm with relative intensity $[\Theta]_{222}/[\Theta]_{207} \approx 0.4$, which is in good agreement with the theoretical value calculated by Manning and Woody[11] for the 3_{10}-helix. The slightly weaker intensity of the positive band at 195 nm, relative to the calculated value, was attributed to the chain length of the sequence, which is too short to form a fully stable helix in solution. These investigations were extended to a series of L-(αMe)Val homo-oligomers with chain lengths ranging from 3−8 residues.[13] The preference toward the helical conformation in solvent systems such as TFE, HFIP (1,1,1,3,3,3-hexafluoro-2-propanol), and HFA (1,1,1,3,3,3-hexafluoroacetone hydrate) increases, as expected, with chain length, but is also concentration-dependent. For instance, in HFIP the octamer at concentration higher than 1 mM exhibits a CD pattern previously attributed to the 3_{10}-helix,[14] while in more dilute solutions the typical CD pattern of the α-helix is observed. Interestingly enough, these authors also observed that the CD spectrum of the concentrated solution is time-dependent and slowly changes into that typical of the α-helix.[14,15] These concentration- and time-dependent phenomena suggest the presence of aggregation under these experimental conditions.

The major problem faced in determining precisely the different spectroscopic properties of the two helical conformations is 2-fold: (1) design of a peptide sequence which can exclusively assume the 3_{10}-helical structure, (2) choice of a solvent system suitable for a combined analysis by NMR and CD in the peptide absorption region. Therefore, we attempted the design of a series of conformationally constrained peptides that will predominantly fold into the 3_{10}-helix.

It has been shown by different authors[16,17] that the intrinsic ability of a given peptide sequence to fold into the α-helical conformation is enhanced when the side chains of Asp(i)−(Lys(i+4) or Glu(i)−(Lys(i+4) are lactam-bridged. Houston et al.[17] determined the effect of ring size and orientation of lactam amide on the peptide conformation. Their findings suggest that the Glu→Lys oriented bridge is more effective than the Lys→Glu bridge in stabilizing the α-helical conformation. On the contrary, the (i)−(i+3) lactam bridge was α-helix-destabilizing. This is in line with the C═O(i)···HN(i+4) intramolecular H-bond scheme of the α-helix. Following the same rationale, the propensity of peptides rich in C^{α}-tetra-substituted amino acid residues to fold into a 3_{10}-helical conformation may be enhanced by the presence of sequences containing Glu(i)−(Lys(i+3) lactam-bridged side chains. In any case, the Glu(i)−(Lys(i+3) lactam bridge is expected to destabilize the α-helical conformer. In the present study we attempt to obtain peptide sequences with a unique conformational preference toward the 3_{10}-helix in solution. We therefore designed and synthesized the following series of Aib-containing peptides constrained by side-chain lactam bridges:

Ac-(Glu-Aib-Aib-Lys)$_1$-Ala-OH (monomer)

Ac-(Glu-Aib-Aib-Lys)$_2$-Ala-OH (dimer)

Ac-(Glu-Aib-Aib-Lys)$_3$-Ala-OH (trimer)

L-Amino acids were used in order to favor the formation of right-handed helices.

To study the effect of main-chain length on the conformational preference and possibly to verify the correlation between far UV chiroptical properties and polypeptide secondary structure, we carried out a detailed CD and NMR analysis in aqueous solution containing SDS (sodium dodecylsulfate) micelles followed by an NOE-distance-based structure ensemble calculations using the XPLOR simulated annealing protocol. As solvent medium we chose the aqueous SDS micellar system, well known to induce ordered secondary structures in relatively short bioactive peptides.[18] This solvent system dissolves relatively hydrophobic peptides and is suitable for both CD and NMR measurements.

Experimental Section

Peptide Synthesis. Fmoc-Aib-Aib-OH. H-Aib-O*t*Bu (3.2 g, 20 mmol) and Fmoc-Aib-OH (6.5 g, 20 mmol) (Fmoc, fluorenylmethyloxycarbonyl) were dissolved in dichloromethane (DCM) (70 mL). Dicyclohexylcarbodiimide (4.12 g, 20 mmol) was added and the mixture stirred at room temperature for 2 h. The solid was filtered off and the filtrate evaporated to dryness. The solid residue was treated with a mixture of anisole (4 mL), water (4 mL), and TFA (trifluoroacetic acid) (100 mL) for 1 h. After evaporation to dryness Fmoc-Aib-Aib-OH was recrystallized from ethyl acetate (AcOEt)/petroleum ether (PE) (1:1). The purity of the product was assessed by TLC [$R_f = 0.34$, PE:AcOEt:AcOH(acetic acid) 50:50:1] and analytical RP-HPLC. The molecular

(11) Manning, M.; Woody, R. W. *Biopolymers* **1991**, *31*, 569−586.
(12) Sudha, T. S.; Vijayakumar, E. K. S.; Balaram, P. *Int. J. Pept. Protein Res*. **1983**, *22*, 464−468.
(13) Yoder, G.; Polese, A.; Silva, R. A. G. D.; Formaggio, F.; Crisma, M.; Broxterman, Q. B.; Kamphuis, J.; Toniolo, C.; Keiderling, T. A. *J. Am. Chem. Soc*. **1997**, *119*, 10278−10285.
(14) Toniolo, C.; Polese, A.; Formaggio, F.; Crisma, M.; Kamphuis, J. *J. Am. Chem. Soc*. **1996**, *118*, 2744−2745.
(15) Mammi, S.; Rainaldi, M.; Bellanda, M.; Schievano, E.; Peggion, E.; Broxterman, Q. B.; Formaggio, F.; Crisma, M.; Toniolo, C. *J. Am. Chem. Soc*. **2000**, *122*, 11735−11736.
(16) Felix, A. M.; Heimer, E. P.; Wang, C. T.; Lambros, T. J.; Fournier, A.; Mowies, T. F.; Maines, S.; Campbell, R. M.; Wegrzynski, B. B.; Toome, V.; Fry, D.; Madison, V. S. *Int. J. Pept. Protein Res*. **1988**, *32*, 441−454.
(17) Houston, M. E.; Cannon, C. L.; Kay, C. M.; Hodges, R. S. *J. Pept. Sci*. **1995**, *1*, 274−282.
(18) Peggion, E.; Mammi, S.; Schievano, E. *Biopolymers (Pept. Sc.)* **1997**, *43*, 419−431.

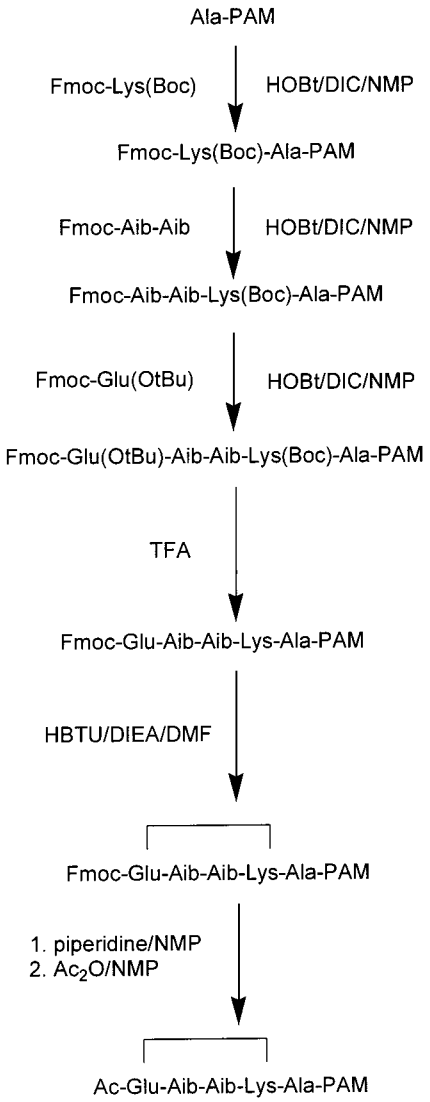

Figure 1. Synthetic scheme followed for the preparation of the monomer.

weight determined by FAB-MS (calculated 410, observed 411 $[M + H]^+$, 433 $[M + Na]^+$, 449 $[M + K]^+$) was consistent with the expected product.

Ac-Glu-Aib-Aib-Lys-Ala-OH, Ac-[(Glu-Aib-Aib-Lys)]$_2$-Ala-OH, and Ac-[(Glu-Aib-Aib-Lys)]$_3$-Ala-OH. The synthetic scheme to prepare the designed monomer is shown in Figure 1. The syntheses were carried out by the solid-phase methodology using the Boc-Ala-PAM resin (Boc, *tert*-butyloxycarbonyl) (1 mM). Deprotection followed by sequential coupling of Fmoc-Lys(Boc)-OH, Fmoc-Aib-Aib-OH, and Fmoc-Glu(O*t*Bu)-OH was performed using HOBt-activated amino acid (4 equiv) in *N*-methylpyrrolidone (NMP). Deprotection of the Fmoc-protecting group was performed with 30% piperidine in NMP. Following completion of the peptide assembly, deprotection of the Boc- and O*t*Bu-protecting groups of Lys and Glu side chains, respectively, was performed with 50% TFA in DCM. Side-chain-to-side-chain cyclization was carried out on the resin using 3 equiv of HBTU (*O*-[(1H-benzotriazol-1-yl)-*N*,*N*,*N*′,*N*′-tetramethyluronium hexafluorophosphate) in *N*,*N*-dimethylformamide (DMF) containing diisopropylethylamine (DIEA) (6 equiv). Following Fmoc removal, the α-amino group of one-third of the resin-bound cyclic peptide was acetylated with acetic anhydride in NMP to yield Ac-(Glu-Aib-Aib-Lys)-Ala-PAM. The remaining resin was used to generate Ac-[(Glu-Aib-Aib-Lys)]$_2$-Ala-OH and Ac-[(Glu-Aib-Aib-Lys)]$_3$-Ala-OH following the same synthetic protocol. The completed resin-bound peptides were cleaved from the resin by treatment with 10% anisole/HF for 75 min at 0 °C. Peptides were purified by RP-HPLC as described by Nakamoto et al.[19] Purity of the peptides (> 99%) was assessed by analytical RP-HPLC. Structural integrity was confirmed by amino acid analysis and electrospray mass spectrometry (ES-MS).

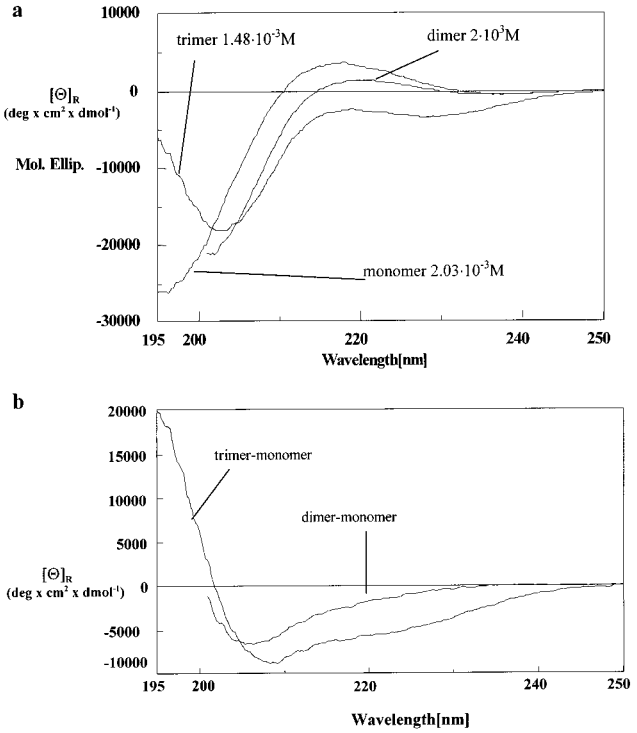

Figure 2. (a) CD spectra of monomer, dimer, trimer in 0.1 M SDS. The peptide concentrations are indicated in the spectra. (b**)** Difference CD spectra dimer *minus* monomer and trimer *minus* monomer (from a).

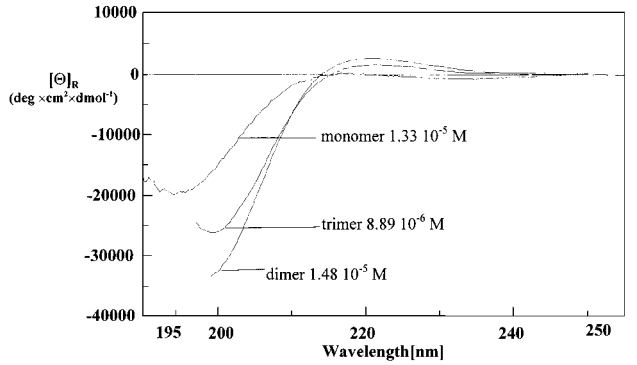

Figure 3. CD spectra of monomer, dimer, trimer in TFE. The peptide concentrations are indicated in the spectra.

CD Measurements. CD measurements were carried out on a JASCO J-715 spectropolarimeter interfaced with a PC. The CD spectra were acquired and processed using the Jasco J-700 program for Windows. All measurements were performed at room temperature using Hellma quartz cells with Suprasil windows and with optical path lengths ranging from 0.02 to 1 cm. The spectra were recorded using a bandwidth of 2 nm and a time constant of 8 s at scan speeds in the range of 20−50 nm/min. Accumulation of 6−8 scans was routinely used in order to improve the signal-to-noise ratio.

NMR Experiments. NMR experiments were carried out on a Bruker AVANCE DMX-600 spectrometer. The peptide concentrations ranged from 1.1 to 8 mM in 0.1−0.2 M SDS-d_{25}. The water signal was suppressed by presaturation during the relaxation delay or by use of

(19) Nakamoto, C.; Behar, V.; Chin, K.; Adams, A. E.; Suva, L. J.; Rosenblatt, M.; Chorev, M. *Biochemistry* **1995**, *34*, 10546−10552.

Table 1. Temperature Coefficients (ppb/K) and Standard Deviations of Residues of the Monomer (a), of the Dimer (b), and of the Trimer (c)

residue	E^1	Aib^2	Aib^3	K^4	A^5
			a		
$\Delta\delta/\Delta T$	−6.5	−6.6	−4.1	−2.6	−4.5
σ	± 0.4	±0.5	±1.2	±0.2	±0.9

residue	E^1	Aib^2	Aib^3	K^4	E^5	Aib^6	Aib^7	K^8	A^9
					b				
$\Delta\delta/\Delta T$	−5.4	−4.5	−3.4	−2.6	−2.4	−0.9	−4.8	−1.7	−2.9
σ	±0.5	±0.3	±0.3	±0.6	±0.17	±0.04	±0.5	±0.9	±1.1

residue	E^1	Aib^2	Aib^3	K^4	E^5	Aib^6	Aib^7	K^8	E^9	Aib^{10}	Aib^{11}	K^{12}	A^{13}
							c						
$\Delta\delta/\Delta T$	−4.4	−3.6	−3.3	−2.5	−2.5	−1.0	−4.0	−2.2	−2.6	−2.0	−3.6	−0.4	−1.6
σ(ppb/K)	±0.4	±0.3	±0.3	±0.4	±0.5	±0.3	±0.5	±0.7	±0.4	±0.5	±0.7	±0.09	±0.5

the WATERGATE[20] pulse sequence. In all homonuclear experiments the spectra were acquired by collecting 500−512 experiments, each one consisting of 64 scans and 4K data points. The spin systems of proteic amino acid residues were identified using standard DQF-COSY[21] and CLEAN-TOCSY[22,23] spectra. In the latter case the spin-lock pulse sequence was 70 ms long. The resonances of all the carbon signals were identified with the following experiments. The assignment of methyl groups belonging to the same Aib residue was obtained by means of 2D $^1H-^{13}C$ correlation spectra. To optimize the digital resolution in the carbon dimension, semisoft HMQC and semisoft HMBC experiments were acquired using selective excitation by means of Gaussian-shaped pulses with 1% truncation.[24,25] The Cβ-selective HMQC experiments[26] were recorded with 120−190 t_1 experiments, of 480 scans and 2K points in F2. Signals due to ^{12}C were suppressed by a BIRD sequence.[27] A spectral width of 10 ppm centered at 25 ppm in F1 was used, yielding a digital resolution of 8−13 Hz/pt prior to zero filling. HMBC experiments[28] with selective excitation in the CO region were performed using a long-range coupling constant of 7.5 Hz, a spectral width in F1 of 15 ppm centered at 174 ppm, 120 t_1 experiments of 1000−1300 scans and 4K points in F2. The digital resolution in F1, prior to zero filling, was 19 Hz/pt.

NOESY experiments were used for sequence specific assignment. To avoid the problem of spin diffusion, the build-up curve of the volumes of NOE cross-peaks as a function of the mixing time was determined first (data not shown). The mixing time of the NOESY experiments used for inter-proton distance determination ranged from 100 to 150 ms, that is in the linear part of the NOE build-up curve. To resolve ambiguous and overlapped NOE peaks arising from low F1 resolution in the normal NOESY experiments (6.4 Hz/pt), semisoft NOESY experiments[29] with digital resolution of 0.7 Hz per point in F1 were acquired. A G4-shaped pulse, centered in the Hα region was used to replace the first 90° hard pulse. To verify the compatibility of the distance values obtained by semisoft NOESY with the restraints extracted from standard NOESY, the effect of offset position in the F1 dimension on the volumes of integrated cross-peaks was examined. The distances extracted from several semisoft NOESY experiments were identical, within an accuracy of 5%, to those of normal NOESY attesting a negligible offset effect. Inter-proton distances were obtained by integration of the NOESY spectra using the AURELIA software package. The calibration was based on sequential NH(*5*)−NH(*6*) proton pairs, set to a distance of 2.6 Å. When peaks could not be integrated because of partial overlap, a distance corresponding to the maximum limit of detection of the experiment (4.0 Å) was assigned to the corresponding proton pair.

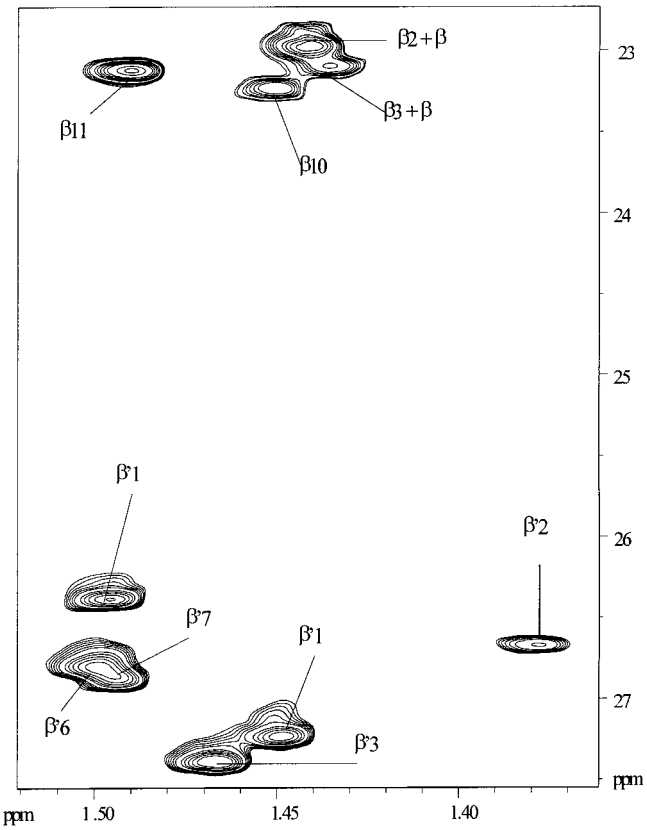

Figure 4. Cβ-selective HMQC spectrum (600 MHz) of the trimer (1.16 mM in 0.199 M SDS-d_{25}).

Structure Calculations. Distance geometry (DG) and molecular dynamics (MD) calculations were carried out using the simulated annealing (SA) protocol of the X-PLOR 3.0 program.[30] For distances involving equivalent or nonstereo-assigned protons, r^{-6} averaging was used. The MD calculations involved a minimization stage of 100 cycles, followed by SA and refinement stages. The SA consisted of 30 ps of dynamics at 1500 K (10000 cycles, in 3 fs steps) and of 30 ps of cooling from 1500 to 100 K in 50 K decrements (15000 cycles, in 2 fs steps). The SA procedure, in which the weights of NOE and nonbonded terms were gradually increased, was followed by 200 cycles of energy minimization. In the SA refinement stage the system was cooled from 1000 to 100 K in 50 K decrements (20000 cycles, in 1 fs steps). Finally, the calculations were completed with 200 cycles of energy minimization using a NOE force constant of 50 kcal/mol. The generated structures

(20) Sklenar, V.; Piotto, M.; Leppik, R.; Saudek, V. *J. Magn. Reson., Ser.* A **1993**, *102*, 241−245.
(21) Rance, M.; Sørensen, O. W.; Bodenhausen, G.; Wagner, G.; Ernst, R. R.; Wüthrich, K. *Biochem. Biophys. Res. Commun.* **1983**, *117*, 479−485.
(22) Bax, A.; Davis, D. G. *J. Magn. Reson.* **1985**, *65*, 355−360.
(23) Griesinger, C.; Otting, G.; Wüthrich, K.; Ernst, R. R. *J. Am. Chem. Soc.* **1988**, *110*, 7870−7872.
(24) Bauer, C.; Freeman, R.; Frenkiel, T.; Keeler, J.; Shaka, A. *J. Magn. Reson.* **1984**, *58*, 442−457.
(25) Emsley, L.; Bodenhausen G. *J. Magn. Reson.* **1989**, *82*, 211−221.
(26) Bax, A.; Griffey, R. H.; Hawkins, B. L. *J. Magn. Reson.* **1983**, *55*, 301−315.
(27) Bax, A.; Subramanian, S. *J. Magn. Reson.* **1986**, *67*, 567−569.
(28) Bax, A.; Summers, M. F. *J. Am. Chem. Soc.* **1986**, *108*, 2093−2094.
(29) Cavanagh, J.; Waltho, J. P.; Keeler, J. *J. Magn. Reson.* **1987**, *74*, 386−393.

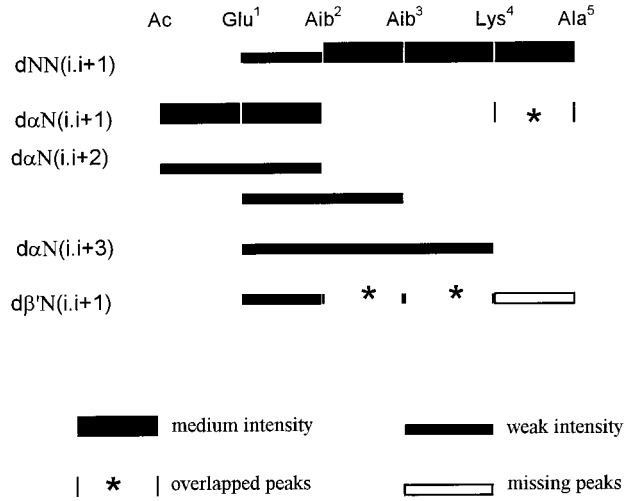

Figure 5. Summary of NOESY connectivities of the monomer (8.0 mM in 0.1 M SDS-d_{25}). Peaks are grouped into two classes based upon their integrated volumes.

were visualized using the INSIGHT II[31] and MOLMOL[32] (version 2.6) programs with a Silicon Graphics O2 R 10000 work station.

Results and Discussion

CD Results. Initially, we investigated the conformational properties of the three oligopeptides by CD in different solvent systems. The CD spectra in 0.1 M SDS are shown in Figure 2. All spectra are independent of peptide concentration in the range $(2 \times 10^{-3})-(2 \times 10^{-5}$M) (data not shown). The spectrum of the monomer exhibits the shape usually associated with the unordered conformation and characterized by a weak positive band at ∼218 nm and a strong negative band at ∼195 nm. Upon chain elongation to the dimer, there is a decrease of the intensity and a red-shift of the CD spectrum. This trend continues in the trimer with a spectrum characterized by a weak negative band around 230 nm ($[\Theta]_R = 4000$ residue molar ellipticity units) and by a strong negative band at ∼203 nm ($[\Theta]_R = 17\,000$ residue molar ellipticity units). These spectral changes are indicative of an increase of ordered conformation upon increasing the length of the peptide chain. On the basis of these CD characteristics only, the type of ordered structure formed upon chain elongation in this solvent system could not be assessed. In the case of the trimer, which should have the highest content of ordered structure, the shape of the CD pattern vaguely resembles that reported by Toniolo et al.[14] for the 3_{10}-helix of Ac-[L-(αMe)Val]$_8$-O*t*Bu in TFE. However, the CD spectra differ in the intensity of the negative band around 203 nm, which in the trimer is twice that of the corresponding band of the (αMe)-Val octamer. Furthermore, the crossover point located around 200 nm in the (αMe)Val oligomer is well below 195 nm in the case of our trimer.

The increase of fractional helicity with increasing chain length can be visualized by the difference CD spectra (dimer *minus* monomer and trimer *minus* monomer) shown in Figure 2b. The difference spectra also offer the advantage of eliminating possible contributions to the optical activity from the side-chain lactam units although such a contribution seems unlikely. In fact, no perturbation of the classical CD pattern of the α-helix was observed in α-helical peptides containing Glu(*i*)−(Lys(*i*+4)

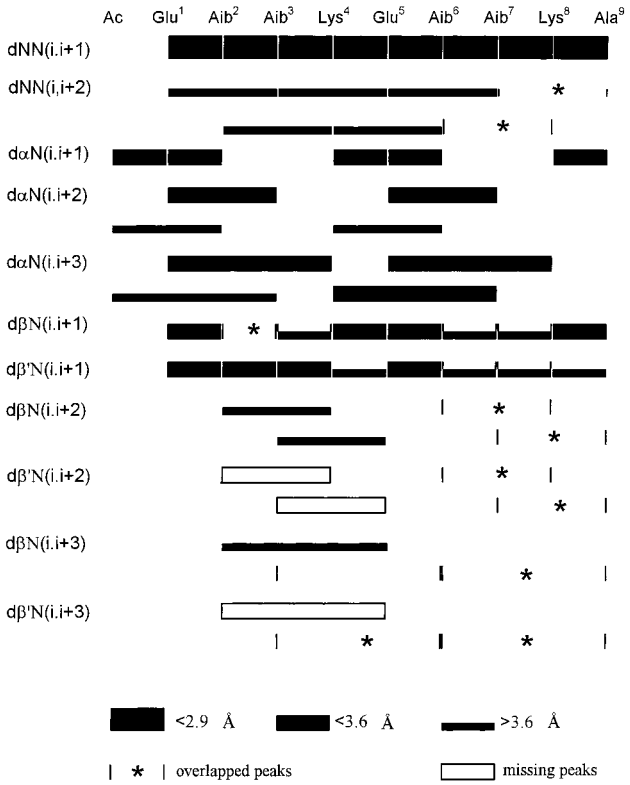

Figure 6. Summary of NOESY connectivities of the dimer (2.23 mM in 0.199 M SDS-d_{25}). Peaks are grouped into three classes based upon their integrated volumes.

lactam-bridged side chains.[17] Helicity clearly increases with main chain length. In particular, the difference CD spectrum trimer *minus* monomer exhibits a negative maximum at 208 nm, an evident shoulder around 220 nm and a positive maximum below 195 nm and the ratio $[\Theta]_{222}/[\Theta]_{207}$ is about 0.65. These spectral features have been observed in many systems where a coil−α-helix equilibrium is present and also in the difference spectrum observed upon the addition of an Aib residue to a partially helical peptide.[9]

The chiroptical properties of the three peptides were also studied in TFE (Figure 3). At a peptide concentration of the order of 1×10^{-5} M the CD spectra of the three peptides share a common shape with a weak positive absorption at 220 nm and a strong negative band at 195−200 nm. In particular, upon chain elongation from the monomer to the trimer, the negative band shifts to the red from ∼195 nm to ∼200 nm. Different from what observed in the SDS-micellar system, the spectra in TFE are concentration-dependent, with the negative maximum increasing in intensity at lower concentrations (data not shown). These results are reminescent of the concentration dependence reported previously for L-(αMe)Val homo-oligomers in organic solvents and suggest that there is a concentration-dependent conformational change consequent to intermolecular aggregation.

NMR Results. A detailed conformational characterization of the three Aib-rich, lactam-bridged cyclic peptides was carried out by 2D-NMR spectroscopy. This study was performed in aqueous solution in the presence of SDS micelles where the peptides exhibit a higher propensity to fold into an ordered structure as indicated by CD. The CD spectra of the solutions used for NMR experiments (∼1 mM) are identical to those recorded at the lower concentrations (data not shown), indicating that the conformation does not change with concentration. For each peptide the spin systems of Glu, Lys, and Ala residues

(30) Brunger, A. T. *X-PLOR Manual* (version 3.0); Yale University: CT, 1992.
(31) *Insight II User Guide*; Biosym/MSI: San Diego, 1995.
(32) Koradi, R.; Billeter, M.; Wüthrich, K. *J. Mol. Graphics* **1996**, *14*, 51−55.

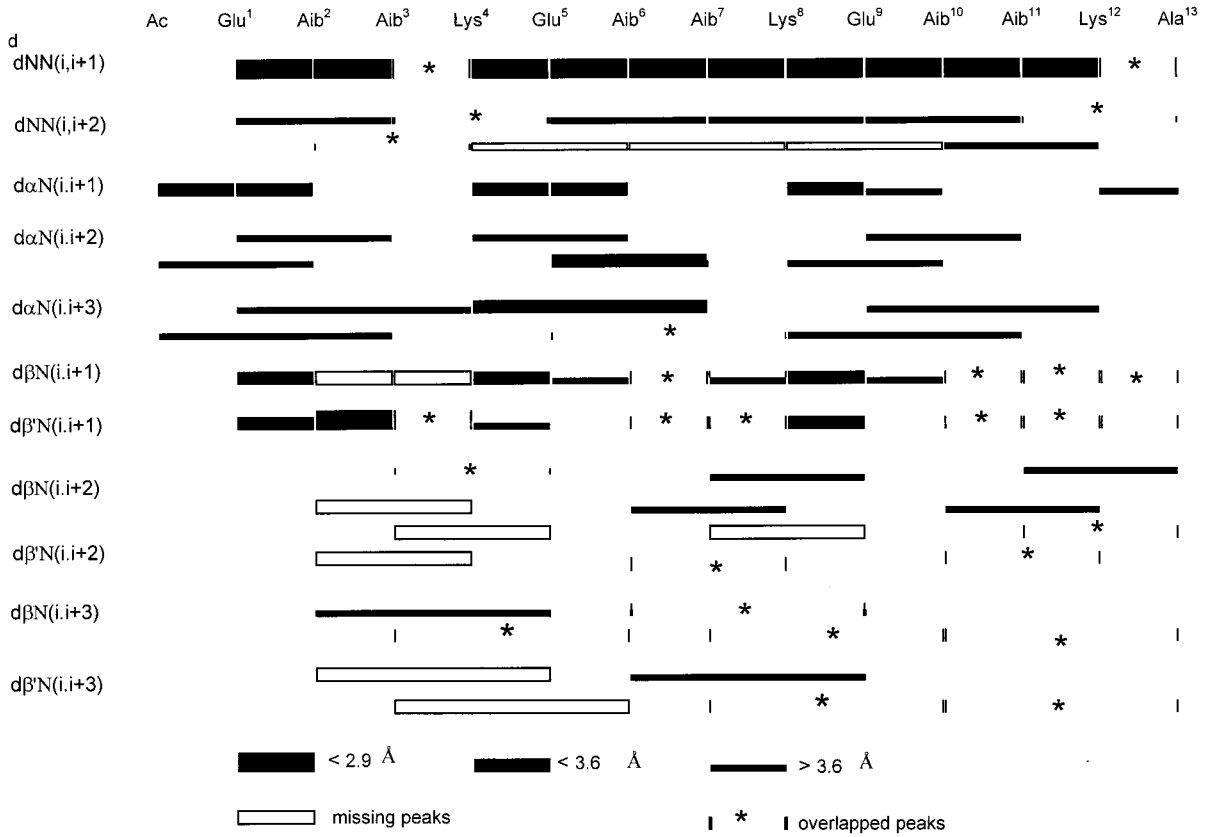

Figure 7. Summary of NOESY connectivities of the trimer (1.16 mM in 0.199 M SDS-d_{25}). Peaks are grouped into three classes based upon their integrated volumes.

Table 2. Chemical Shift of $^{13}C_\beta$ of Methyl Groups of Aib Residues of the Monomer (a), of the Dimer (b), and of the Trimer (c) and Corresponding Values of CNE[31] [a]

residue	$\delta C_{\beta'}H_3$ (ppm)	$\delta C_\beta H_3$ (ppm)	CNE (ppm)
		a	
Aib^2	25.72	23.40	2.31
Aib^3	26.62	23.52	3.09
residue	$\delta C_{\beta'}H_3$ (ppm)	$\delta C_\beta H_3$ (ppm)	CNE (ppm)
		b	
Aib^2	26.51	23.01*	3.50
Aib^3	27.16	23.01*	4.15
Aib^6	26.37	23.37	3.00
Aib^7	27.26	23.26	4.00
residue	$\delta C_{\beta'}H_3$ (ppm)	$\delta C_\beta H_3$ (ppm)	CNE (ppm)
		c	
Aib^2	26.68	22.98**	3.7
Aib^3	27.39	23.10*	4.29
Aib^6	26.88	23.10*	3.78
Aib^7	26.86	22.98**	3.88
Aib^{10}	26.38	23.24	3.14
Aib^{11}	27.23	23.12	4.11

[a] Asterisks indicate overlapped signal.

Table 3. NOE Constraints, Deviations from Idealized Geometry, Mean Energies for the NMR-Based Structures

	dimer	trimer
	no. of NOEs	
total	117	144
intraresidue	49	64
sequential	34	35
$i,i+n$, $n = 2, 3$	34	45
	mean rmsd from ideality of accepted structures	
bonds (Å)	0.007	0.008
angles (deg)	1.01	1.01
improper (deg)	0.53	0.68
NOEs (Å)	0.11	0.13
	mean energies (kcal/mol) of accepted structures	
$E_{overall}$	124.6	206.8
E_{bond}	6.7	13.1
E_{angle}	40.1	57.4
E_{NOE}	68.2	118.1

were identified using DQF-COSY and TOCSY spectra, while HMQC and HMBC experiments were used for the Aib residues. The sequential assignment was performed using NOESY spectra. Important regions of the NOESY spectra are reported in Figures 1−3 of Supporting Information.

The proton chemical shift assignment of the three peptides are reported in Tables 1−3 of the Supporting Information. The temperature coefficients of all amide protons are reported in Table 1. An example of a Cβ-selective HMQC, $^1H-^{13}C$ correlation experiment is shown in Figure 4. The summary of NOE connectivities observed in the three peptides are shown in Figures 5−7. Peaks indicated with asterisks were completely overlapped, and their presence cannot be established unequivocally. These peaks were not used in the structural calculations discussed in the next section. In the case of the monomer, all NH−NH sequential connectivies are present, as well as the αH-(i)−NH(i+2) and αH(i)−NH(i+3) connectivities involving Glu^1. These results are consistent with the onset of some 3_{10}-helical character. However, the relative intensities of αH(1)−NH(2) and αH(1)−NH(4) NOEs indicate that the conformation is not purely helical. NOE connectivities were also observed between the ϵNH proton of Lys^4 and the side-chain protons of Glu^1, clearly due to their proximity in the lactam structure.

In the case of the dimer, there is an increase in the number of sequential and medium-range connectivities, indicative of an ordered conformation. In particular, the observed connectivities

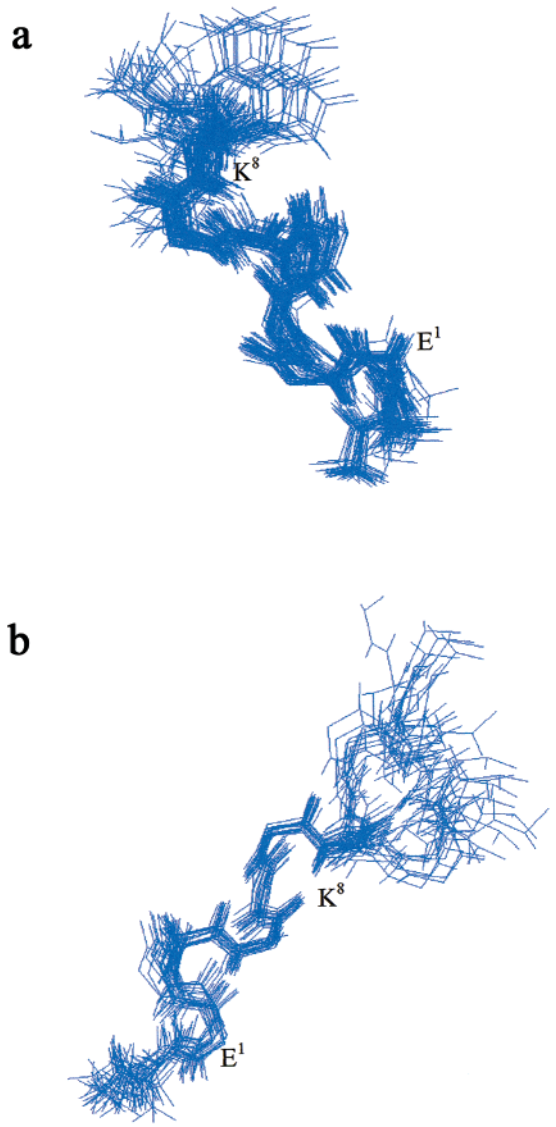

Figure 8. Backbone representation of the 90 structures resulting from MD calculations of dimer, with the backbone atoms in the sequence Glu[1]-Lys[8] superimposed (a). Backbone representation of the 20 structures resulting from MD calculations of trimer with the backbone atoms of residue Glu[1]-Lys[8] superimposed (b).

are of the type αH(*i*)−NH(*i*+2) and αH(*i*)−NH(*i*+3), while no (*i*)−(*i*+4) cross-peak was detected. These results indicate that the conformational preference of the dimer is toward the 3_{10}-helix.

The NOE pattern of the trimer is also consistent with the presence of a 3_{10}-helical conformation. Indeed, even if the αH(1)−NH(3), αH(8)−NH(10), and αH(9)−NH(11) cross-peaks could not be integrated because of partial overlap, all possible αH(*i*)−NH(*i*+2) connectivities are present. A number of the expected (*i*)−(*i*+3) cross-peaks are also present, while no (*i*)−(*i*+4) cross-peaks, indicative of an α-helix, were observed. All of these data support the presence of the 3_{10}-helical conformation. The relative intensities of the (*i*)−(*i*+3) versus (*i*)−(*i*+1) NOEs suggest a substantial helix population but does not exclude the presence of some unfolded conformers.

Further indication of the increase of ordered structure with chain elongation arises from the temperature coefficient of the amide proton resonances, reported in Table 1. It is generally assumed that NHs with temperature gradients less negative than −3 ppb/°C are solvent-shielded, provided that the peptide structure is stable within the explored temperature range. In the case of the monomer, the temperature coefficient of the amide proton of Lys[4] is in the range usually observed for H-bonded NH groups. In the case of the dimer, with the exception of Aib[7], temperature coefficients indicative of the presence of H-bonded NH groups are observed in the entire C-terminal sequence starting from Lys[4]. In the trimer, with the exception of Aib[7] and Aib[11], the temperature coefficients indicate the presence of an H-bonded structure spanning the entire sequence. In the three examined peptides a clear pattern of temperature coefficients is observed within the lactam-bridged structures. The NH of the second Aib displays a higher temperature coefficient than that of the neighboring residues (Aib[2] is never H-bonded since it is at the beginning of the sequence). This repetitive feature, observed in Aib[3], Aib[7], and Aib[11], might imply that the H-bond scheme of the 3_{10}-helix is locally perturbed by a constraint introduced by the lactam bridge.

Finally, the presence of helical structures in the micellar solution was also demonstrated by heteronuclear experiments. The two methyl groups in Aib residues belonging to chiral peptides are diastereotopic, with the *pro-R* group corresponding to the Hα position of L-amino acids and the *pro-S* group to the side chain. Consequently, the carbon atoms of the two methyl groups are chemically non-equivalent and therefore have two different chemical shifts (labeled as *β* and *β′*), above and below 25 ppm (Figure 4**)**.

It has been shown by Jung et al.[33] that the presence of a chiral group adjacent to two gem-methyl groups as in an Aib residue induces a chemical shift difference between these pro-chiral methyls not higher than 0.5 ppm. However, a difference in ^{13}C chemical shifts (termed chemical non-equivalence, CNE) of the two pro-chiral methyls of 2 ppm or higher has been ascribed to the presence of a stable helical conformation in solution. In Table 2, the CNE for the Aib residues in the three oligomers, measured in C*β*-selective HMQC experiments, are reported. All values are higher than 2 ppm, confirming again the existence of ordered structures in SDS solution. The increase of structural order upon peptide chain elongation is also evident from the increase of CNE values.

It is possible to achieve the stereospecific assignment of the two diastereotopic methyls by analyzing the different intensity of NOE cross-peaks of the type *β*N(*i*,*i*+1), *β*N(*i*,*i*+2), and *β*N(*i*,*i*+3).[34] In our spectra, a comparison of the intensity of these cross-peaks was possible only for the methyls of Aib[2], in both the dimer and the trimer. For this residue, the methyl groups which resonate at lower fields in the carbon dimension are *pro-S* because they do not present cross-peaks of the type *β*N(*i*,*i*+2) and *β*N(*i*,*i*+3). This result is consistent with the data reported by Bellanda et al.[34] Unfortunately, peak overlap in the NOESY spectra did not allow the stereospecific assignment of the other methyl groups, and consequently this information was not available for the molecular dynamics simulations.

Structure Calculations. The conformational properties of the oligomers were further investigated by DG and restrained MD calculations. The calculations were limited to the dimer and trimer for which a sufficient number of inter-proton distances was available. A total of 117 and 144 inter-proton distance restraints for the dimer and trimer, respectively, were derived from NOESY spectra and used in the SA protocol. In the case of the dimer, 90 structures were generated with NOE violations lower than 0.5 Å (Table 3); the average pairwise root-

(33) Jung, G.; Brückner, H.; Bosch, R.; Winter, W.; Schaal, H.; Strähle, J. *Liebigs Ann. Chem.* **1983**, 1096−1106.

(34) Bellanda, M.; Peggion, E.; Bürgi, R.; van Gunsteren, W.; Mammi, S. *J. Pept. Res.* **2001**, *57*, 97−106.

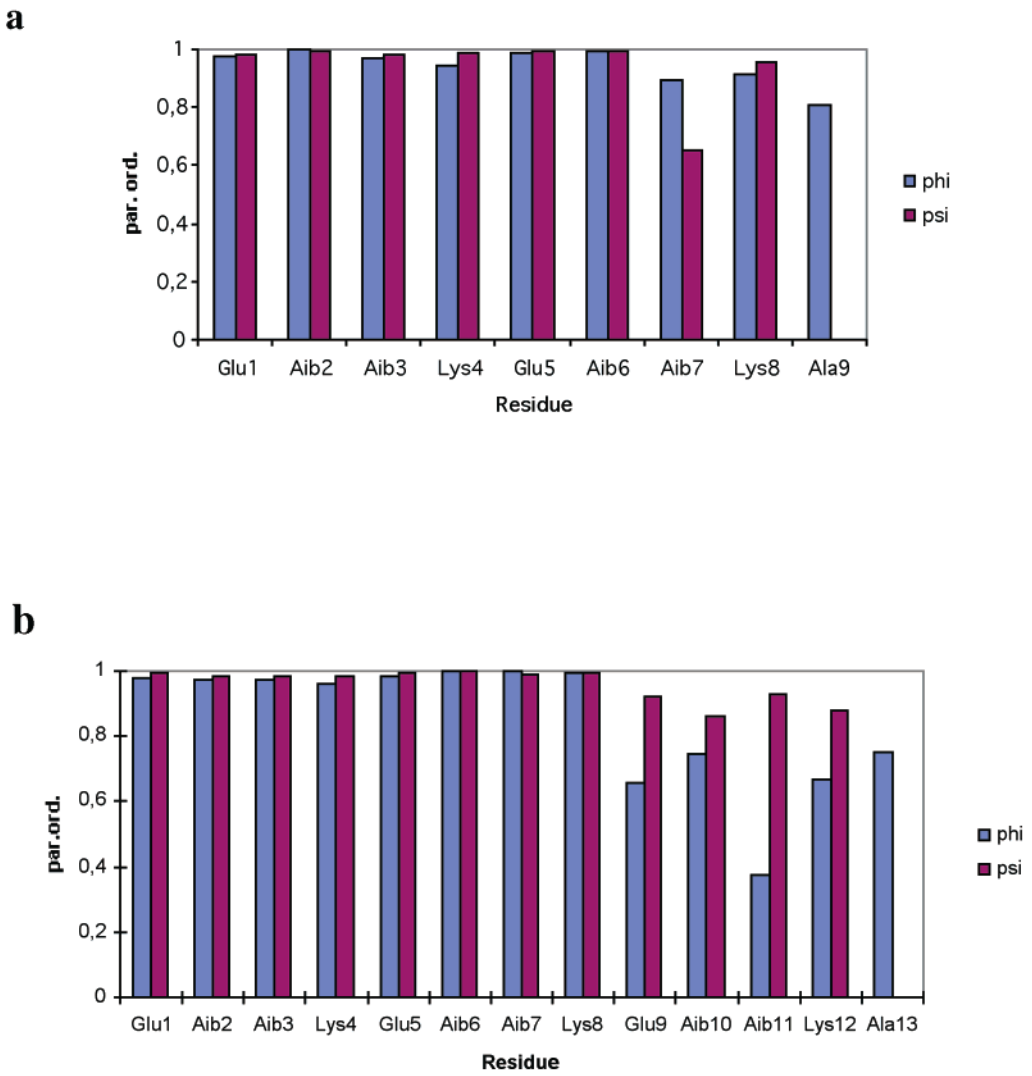

Figure 9. Order parameter values of the backbone dihedral angles ϕ, ψ calculated from the ensembles of structures obtained by MD calculations of dimer (a) and trimer (b).

mean-square deviation (rmsd) of backbone atoms was 1.3 ± 0.5 Å. In the case of the trimer, 20 structures with violations lower than 0.5 Å were generated, with a backbone average pairwise rmsd of 0.7 ± 0.2 Å.

The superposition of the ensemble of the low-energy structures of the two peptides are shown in Figure 8. The order parameters of the backbone dihedral angles extracted from these ensembles are shown in Figure 9. The results indicate that all structures converge to a well-defined helical conformation comprising the sequences Glu[1]-Aib[6] in the dimer and Glu[1]-Lys[8] in the trimer, while the conformations of the C-terminal portions of both oligomers seem to be less defined. A possible reason for this result could be the lower number of inter-proton distance restraints available in these regions of the sequence, due to NOESY cross-peaks overlap.

The average values of the torsion angles and the relative standard deviations resulting from the low-energy structures of the two sequences are reported in Table 4. The ϕ and ψ dihedral angles of α- and 3_{10}-helices differ only by 6° and 12° respectively.[2] Since the standard deviations from the average of the ϕ angles are well above the 6° difference between the 3_{10}-helix and the α-helix, from the average values it is not possible to distinguish between the two structures. However, the values of the ψ dihedral angles are in general lower than 42° typical of the α-helix, and in many cases they are close to

Table 4. Average Values of Torsion Angles and the Relative Standard Deviations Resulting from the 90 Calculated Structures of Dimer (a) and from the 20 Calculated Structures of Trimer (b)

residue	ϕ	$\Delta\phi$	ψ	$\Delta\psi$
		a		
Glu[1]	− 65.6	± 15.2	−37.0	± 11.7
Aib[2]	− 45.3	± 4.5	−26.8	± 5.1
Aib[3]	− 77.9	± 14.3	−31.4	± 11.1
Lys[4]	− 78.8	± 19.7	−14.8	± 10.0
Glu[5]	− 84.6	± 8.2	−23.0	± 7.4
Aib[6]	− 57.1	± 6.2	−33.4	± 5.9
Aib[7]	−105.7	± 27.0	− 3.4	± 51.1
Lys[8]	− 60.5	± 25.7	−21.1	± 16.9
Ala[9]	−121.5	± 42.8		
		b		
Glu[1]	−59.7	± 12.5	−36.8	± 7.1
Aib[2]	−52.1	± 14.3	−23.5	± 10.8
Aib[3]	− 68.1	± 13.9	−28.0	± 10.5
Lys[4]	− 79.8	± 16.4	−36.6	± 11.2
Glu[5]	− 71.4	± 11.1	−22.4	± 4.6
Aib[6]	− 51.8	± 3.5	−28.6	± 1.8
Aib[7]	− 57.2	± 3.0	−35.5	± 8.8
Lys[8]	− 71.8	± 7.1	−22.3	± 6.6
Glu[9]	− 17.7	± 50.6	− 3.9	± 23.7
Aib[10]	− 9.5	± 42.8	− 1.6	± 31.5
Aib[11]	− 14.3	± 70.6	+ 3.2	± 22.7
Lys[12]	− 0.2	± 49.7	−43.1	± 29.6
Ala[13]	−110.3	± 42.9		

Table 5. Probability of CO(*i*)···HN(*i*+3) and CO(*i*)···HN(*i*+4) Intramolecular Hydrogen Bonds of Amide Protons in the Calculated Structures of the Dimer (a) and the Trimer (b)[a]

residue	Aib[3]	K[4]	E[5]	Aib[6]	Aib[7]	K[8]	A[9]
			a				
H-bond (*i*,*i*+3)	32%	100%	39%	30%	4.4%	48.8%	
H-bond (*i*,*i*+4)			11.1%	7.8%			21.1%

residue	Aib[3]	K[4]	E[5]	Aib[6]	Aib[7]	K[8]	E[9]	Aib[10]	Aib[11]	K[12]	A[13]
					b						
H-bond (*i*,*i*+3)	55%	75%	35%	25%	50%	95%	65%	35%	80%	100%	55%
H-bond (*i*,*i*+4)			5%	35%							

[a] The maximum hydrogen-acceptor distance was set to 2.4 Å, and the donor−hydrogen−acceptor bond angle was = 145°.

the value of 30° characteristic of the 3_{10}-helix, with standard deviations lower than 12° (for residues 1−8).

The population of C═O(*i*)- - -HN(*i*+3) H-bonds, indicative of a 3_{10}-helix, in the low-energy structures can be calculated from the coordinates of the carbonyl oxygen and amide hydrogen atoms. The H-bond pattern clearly indicates the preference for (*i*)−(*i*+3) H-bonds in both peptides (Table 5) and therefore supports the conclusion that the preferred conformation of the two peptides is the 3_{10}-helix. In the case of the dimer, this H-bond pattern comprises the sequence from Aib[3] to Lys[8], with an interruption at Aib.[7] In the case of the trimer, the (*i*)−(*i*+3) H-bond pattern is highly preferred throughout the entire sequence starting from Aib[3]. The reduced probability of H-bonds for at least one Aib NH in each lactam-bridged cycle (Aib[7] in the dimer, Aib[7] and Aib[10] in the trimer) is again a possible indication of a slight strain in the 3_{10}-helical conformation caused by the lactam bridge.

Conclusions

The results presented in this paper show that the Aib-rich oligomers constrained by Glu(*i*)−Lys(*i*+3) side-chain-to-side-chain lactamization, which destabilizes the α-helical structure, tend to assume the 3_{10}-helical conformation upon chain elongation. A number of αH(*i*)−HN(*i*+2) connectivities were identified in the NOESY spectra of the three peptides. The presence of the 3_{10}-helix was further supported by the temperature coefficients of the NH proton chemical shifts which are in the range usually observed in an H-bonded structure and, most important, by the high probability for (*i*)−(*i*+3) H-bond pattern in the calculated structures. However, the CD properties change with main chain elongation and, in particular, the difference CD spectra of dimer *minus* monomer and trimer *minus* monomer clearly indicate an increase of helicity with chain length. The combined CD and NMR analyses, carried out in the same solvent, indicate that for each peptide we are dealing with equilibrium systems in which conformers with different transient secondary structures are in a rapid exchange on the NMR time scale. In a system of peptide molecules with different transient secondary structure content in a fast dynamic equilibrium, the medium-range NOE data tend to overemphasize the helix content. According to our interpretation, the change of the CD pattern with chain elongation reflects the shift of the conformer equilibrium, from a predominantly random structure in the monomer toward an increasing population of helical molecules in the dimer and the trimer. Based upon this assumption, the difference CD spectra shown in Figure 2b should correspond to the CD spectrum of the ordered structure formed upon chain elongation, that is, the 3_{10}-helix. However, the double negative maximum difference CD spectrum trimer *minus* monomer does not match the putative CD spectrum of the 3_{10}-helix reported in the literature.[14] In particular, the ratio of molar ellipticities $[\Theta]_{222}/[\Theta]_{208}$ is of about 0.65, and is higher than the value of 0.4 reported in the literature.[14]

A possible reason for these differences could rest on a different equilibrium of the conformer population in the various solvent media used in the different studies. If the conformer equilibrium is not completely shifted toward the 3_{10}-helix, the requirement that the designed peptide sequence adopts exclusively such a structure is not fulfilled. In such a case, the CD spectrum would be obviously determined by the contribution of random and ordered structures. Conformational studies on oligomers of Aib or, in general, of C^{α}-tetra-substituted amino acid residues, carried out in different laboratories,[1−8,35] seem to indicate that the 3_{10}-helix is fully developed in solution already at the level of the octapeptides. On the other hand, sequence longer than dodecapeptides rich in C^{α}-tetra-substituted amino acid residues, but containing also proteic amino acids, seem to prefer the α-helix. The 13-residue sequence of the trimer studied in the present work does not show any conformational preference toward the α-helix. Thus, the introduction of the lactam-bridge constraints was successful in enhancing the conformational preference toward the 3_{10}-helix. On this basis we conclude that in the trimer the conformer equilibrium in the solvent system used in the present work is substantially shifted toward the 3_{10}-helix.

To solve unambiguously the problem of differentiation of 3_{10}-helices from α-helices by electronic CD, further work will be directed to the design of peptides with improved, unique conformational preference for the 3_{10}-helix in solvent systems suitable for a combined CD and NMR analysis. Extension of our studies to lactam-constrained oligomers of the series examined in the present work with higher chain length and comparison with the corresponding linear sequences will certainly contribute to solving the problem of the full characterization of the 3_{10}-helix. Work in this direction is in progress in our laboratory.

Acknowledgment. We are grateful to Professor Claudio Toniolo and Professor Fernando Formaggio (Department of Organic Chemistry, University of Padova) for discussions and critical reading of the manuscript. Particular thanks are due to Professor Niels Andersen (Chemistry Department, University of Washington, Seattle) for the suggestions and help in preparing the revised manuscript. The financial support of Consiglio Nazionale delle Ricerche (C.N.R.) of Italy is gratefully acknowledged.

Supporting Information Available: The proton chemical shifts of the three peptides are reported in Tables 1−3; examples of NOESY spectra of the three peptides are reported in Figures 1−3 (PDF). This material is available free of charge via the Internet at http://pubs.acs.org.

JA0027261

(35) Toniolo, C.; Bonora, G. M.; Barone, V.; Bavoso, A.; Benedetti, E.; Di Blasio, B.; Grimaldi, P.; Lelj, F.; Pavone, V.; Pedone, C. *Macromolecules* **1985**, *18*, 895−902.